ORIGINAL RESEARCH

Moisture as key for understanding the fluorescence of lignocellulose in wood

Frank B. Peters · Andreas O. Rapp

Abstract The fluorescence behaviour of lignocellulose in *Pinus sylvestris* L. was studied under the influence of moisture. Fluorescence excitation-emission-matrices (EEMs) of the solid wood surfaces were recorded. Two emission peaks were identified, one attributed to lignocellulose, the other to pinosylvins. The two peaks were successfully modelled with PARAFAC2-deconvolution. Lignocellulose showed excitation-dependent emission. Its emission was quenched and blue-shifted by moisture, while pinosylvin showed none of these properties. The quenching efficiency was proportional to the moisture content (linear Stern–Volmer plot), a phenomenon first demonstrated for wood in this study. Potential mechanisms for the moisture quenching are discussed, with clustering-triggered emission best explaining most of the observed peculiarities. The strong influence of moisture on the fluorescence of pine wood suggests that carbohydrates, or interactions between carbohydrates and lignin, play an important role in lignocellulose fluorescence.

Keywords Moisture · Lignocellulose · Fluorescence quenching · FRET · EEM · Clustering-Triggered emission

F. B. Peters (✉) · A. O. Rapp
Institut Für Berufswissenschaften Im Bauwesen, Leibniz-Universität Hannover, Herrenhäuser Straße 8, 30419 Hannover, Germany
e-mail: peters@ibw.uni-hannover.de

Abbreviations

SD	Standard deviation
EEM	Excitation emission matrix
FRET	Förster resonance energy transfer
Ex	Excitation wavelength
Em	Emission wavelength

Introduction

Relevance of lignocellulose fluorescence

Given the increasing importance of biorefinery and the urgent need for sustainable resource utilization, it is highly relevant to understand the complexity of natural materials, in particular with regards to quality and process control. Fast, cheap and non-destructive analysis methods are needed to fully exploit the potential of the resources for the diverse applications (Galkin et al. 2017).

Several approaches have been made to use fluorescence spectroscopy for species identification on solid wood (Camorani et al. 2008; Ma et al. 2023; Moya et al. 2013; Piuri and Scotti 2010) and wood extracts (Pandey et al. 1998). Fluorescence imaging has been used for heartwood detection (Antikainen et al. 2012), photodegradation monitoring (Peters and Rapp 2021) and various identification and classification applications in microscopy (Babi 2017; Chimenez et al. 2014; Donaldson and Vaidya 2017; Maceda and Terrazas 2022; Mishra et al. 2018; Selig

et al. 2012). Fluorescence lifetime imaging has been proposed for the classification of waste wood (Leiter et al. 2022) and for the analysis of lignin in compression wood (Donaldson and Radotic 2013) and sugar bagasse (Coletta et al. 2013).

In contrast to the above qualitative or semi-quantitative approaches, exact quantitative fluorescence-based methods on solid lignocellulosics are rare. Belt et al. (2021) proposed UV-excited fluorescence spectroscopy for quantitative measurements of stilbene content in pine wood. The correlation between fluorescence intensity and stilbene content was rather weak (r = 0.79). Werner and Pecina (1995) proposed fluorescence spectroscopy as a useful method for the quantitative monitoring of mass loss by fungal attack in beech wood, although their results showed high statistical variation.

It must be considered that fluorescence spectroscopy of solid surfaces is generally subject to higher errors than in liquids. These errors include internal filter effects, light absorbing extractives, quenching effects, surface roughness, and others. In general, it can be said that fluorescence spectroscopy of solids is less common, and some influencing factors are not yet fully understood. A better knowledge of the mechanisms of wood fluorescence will help to reduce these errors and increase the applicability of fluorescence methods in solid wood.

Attribution of lignocellulose fluorescence peaks to chemical substances

A fundamental question is the source of general wood fluorescence. In this context, the general fluorescence of lignocellulose has to be clearly separated from the strong fluorescence reported for specific wood species (Avella et al. 1988), originating from individual fluorophore extractives. Surprisingly, there is no consensus in the research community about the chemical compounds nor the mechanisms contributing to the general fluorescence spectra of lignocellulose. A number of studies have explained the general fluorescence of the wooden cell wall with the distribution and composition of lignin (Auxenfans et al. 2017; Chabbert et al. 2018; Djikanović et al. 2007; Donaldson 2013; Donaldson et al. 2015; Donaldson and Knox 2012; Ji et al. 2013). Also, a recent review of the autofluorescence in plants (Donaldson 2020) reports lignin to be a major contributor to wood

fluorescence, with highly excitation-dependent emission. Donaldson (2013) measured blue emission in pine and poplar wood upon UV (355 nm) excitation, green emission upon blue (488 nm) excitation, and red emission upon excitation with green (561 nm) light. This excitation-dependent emission behaviour is uncommon for most fluorophores (Kasha 1950).

On the other hand, cellulose and other cell wall carbohydrates have been shown to emit in a similar range to lignin, also with excitation-dependent emission (Ding et al. 2020). Fluorescence emission of cellulose nanofibres has been reported in the red and infrared range upon green (532 nm) excitation, as well as in the green range upon blue (450 nm) excitation (Khalid et al. 2019), and blue emission upon UV (320 nm) excitation (Castellan et al. 2007; Olmstead and Gray 1997). Also, lignin and cellulose have both been reported to show pH-dependent emission (Donaldson (2013) and Ding et al. (2020), respectively), with lowest emission at pH 7.

Since cellulose does not have delocalized pi-electrons or other conventional fluorescence systems, impurities of different kinds have been assumed to be the source of cellulose fluorescence (Atalla and Nagel 1972; Lloyd and Miller 1979), but it seems very unlikely that the same impurities exist in all kinds of cellulose of different origins and preparation processes. Note that Ding et al. (2020) and Olmstead and Gray (1997) used, among others, bacterial cellulose where lignin cannot at all occur, not even in trace amounts. Despite this striking evidence, the intrinsic fluorescence of cellulose and hemicelluloses often remains unconsidered, when all fluorescence is attributed to lignin only (Auxenfans et al. 2017; Chabbert et al. 2018; Chimenez et al. 2014; Donaldson and Radotic 2013; Hoque et al. 2023).

These contradictions in the above mentioned studies suggest that the true origin of lignocellulose fluorescence is still not fully understood. The apparent parallels between suggested lignin and cellulose fluorescence raise the question of their respective contribution to the fluorescence of native wood.

Unfortunately, lignin is always more or less modified when extracted from wood, and does not exist in pure form without cellulose and hemicelluloses. To examine the fluorescence of native lignin in wood, indirect methods have to be used. The approach of this study was to use moisture as a reversible and non-destructive way of modulating wood fluorescence,

since water is a known fluorescence quencher (Fürstenberg 2017; Maillard et al. 2020) and binds to hydroxyl groups in wood. These groups are especially present in hemicelluloses and cellulose, while lignin is much more hydrophobic (Christensen and Kelsey 1959; Fredriksson et al. 2023; Hou et al. 2022). The aim of this study was therefore to investigate the influence of moisture on the fluorescence of native wood. The results shall contribute to a deeper understanding of the origins of wood fluorescence, and to a better applicability of fluorescence based methods on wood.

Material and methods

Seven samples (axial length x tangential width x radial depth $= 15 \times 15 \times 30$ mm) of commercial Scots pine (*Pinus sylvestris* L.) heartwood were produced with growth ring orientation along the measured surface. The samples were made in axial order from the same annual ring of a wooden strip. The tangential surface was cut down with a razorblade to exclusively examine latewood. Samples were marked one to seven in axial order and stored in darkness at 20 °C at relative humidities of 0, 33, 53, 75, 94, and 2×100 %, respectively. After seven days, two replicate fluorescence excitation emission matrices (EEMs) were recorded from different spots of each sample. In a desorptive approach, this process was repeated for every moisture stage and sample. Photodegradation and other aging processes as cause of variation were ruled out by a final examination of all samples in the first moisture stage. This final examination did not differ significantly from the initial one. Altogether, 112 EEMs were recorded (2 replicates × 7 samples × 7 moisture stages + 14 final measurements).

All EEMs were taken in front-face geometry with a resolution of 5 nm with a Hitachi F-7100 fluorescence spectrometer. An in-house modified beam path setup was used, where the excitation beam impinged on the sample surface at an angle of 34° to the emission lens. The illuminated surface was app. 78 mm^2. By this modification, the ratio of fluorescence signal to higher-order scattering was increased about sixfold, compared to unmodified setup, due to the reduced reflection into the emission lens. After the last measurement, the samples were again stored for 50 days in the respective humidity stages. Then the equilibrium wood moisture was determined according to formula 1.

Formula 1: Wood moisture:

$$u = (m_1 - m_0)/m_0 * 100\%$$

where u is the wood moisture, m_1 is the mass of the moist specimen, and m_0 is the mass of the dried specimen. m_0 was obtained by dring the samples at 60 °C until equilibrium, followed by drying at 103 °C for two hours. This method was reported by Rapp and Sudhoff (2020) to reduce the evaporation of resin in Scots pine and other species with volatile extractives.

The contributions of the individual peaks to the total spectrum were calculated with PARAFAC2 deconvolution in Matlab, using the PLS toolbox (version 9.0) from Eigenvector Research, Inc., Manson, USA. PARAFAC2 was used because of its ability to handle small deviations from trilinearity (Harshman 1972), e.g. retention time shifts in chromatography (Bro et al. 1999), while presenting chemically meaningful information, i.e. pure component spectra (Kiers et al. 1999). To the best of our knowledge, PARAFAC2 was not used before to deconvolute EEMs with compounds that do not follow Kasha's rule (Kasha 1950), i.e. have shifting emission spectra depending on the excitation wavelength. This was the case for the lignocellulose in pine wood, as observed in this study.

A two-component PARAFAC2-model was calculated with constraints set to nonnegativity in concentration and excitation modes. The data was preprocessed in the following steps: Using the EEM filtering tool in the software, Rayleigh scattering signals were removed in first and second orders in a half-width of 35 nm, replacing the missing values by interpolation. All emission signals below the respective excitation wavelength (sub-Rayleigh wavelengths) were set to zero. For the model calculations, the EEMs were clipped to a range of excitation = 250–500 nm and emission = 340–600 nm.

Before interpretation, PARAFAC 2 scores (the calculated "concentration" values) were divided by the peak intensity of kraft paper, stored at 20 °C and 65 % relative humidity, and recorded at the same day after the respective sample. This was done as reference to reduce the influence of long term drifts in lamp intensity and other machine parameters on the spectra. Kraft paper is relatively homogeneous and

Fig. 1 a Typical EEM of pine wood, stored at 0% relative ▶ humidity. One peak (blue arrow) showed excitation-dependent emission. The second peak (red arrow) did not show excitation-dependent emission. (**b**): Emission spectra of a) at excitation wavelengths 395 (blue line) and 325 (red line) nm. (**c**) and (**d**): PARAFAC2 loading surfaces of component 1 and 2, respectively. They represent the deconvolution of the two peaks in a)

shows fluorescence in a wide emission band, comparable to wood.

Results

Identification and characterisation of the fluorescence peaks

The EEMs of pine wood all showed two distinct emission peaks, as exemplified in Fig. 1a. One had a maximum at excitation (Ex) = 385 ± 15 nm and emission (Em) = 458 ± 13 nm (blue arrow/line in Fig. 1a/b) and showed a strong dependence of emission wavelength on excitation wavelength, which can be seen by its diagonal shape in the EEM (Fig. 1a). Note that this excitation-dependent fluorescence emission is unusual because, according to Kasha's rule (Kasha 1950), the emission wavelength of a fluorophore does not depend on excitation wavelength. The second fluorescence peak had a maximum at Ex = 323 ± 8 nm and Em = 413 ± 3 nm (red arrow/line in Fig. 1a/b).

The 2-component PARAFAC2-deconvolution showed promising model details (split-half-analysis: 99.6%; 100% Core consistency; 99.766% explained variance) and successfully deconvoluted the two peaks (Fig. 1c and d).

Changes in fluorescence spectra

Component 1 was considerably quenched by moisture, as displayed in Fig. 2a. Component 2 did not show any significant dependence on water content, but a higher between-sample variance (Fig. 2b). Sample 1, for example, consistently showed higher scores here, while sample 5 had lower scores than average. Additionally, component 2 also showed a high random variance upon repeated measurements.

The quenching efficiency (F_0/F) of each sample was calculated by dividing the intensity in dry condition (F_0) by the intensity of the same sample in the respective moisture stage (F). Figure 3 a and
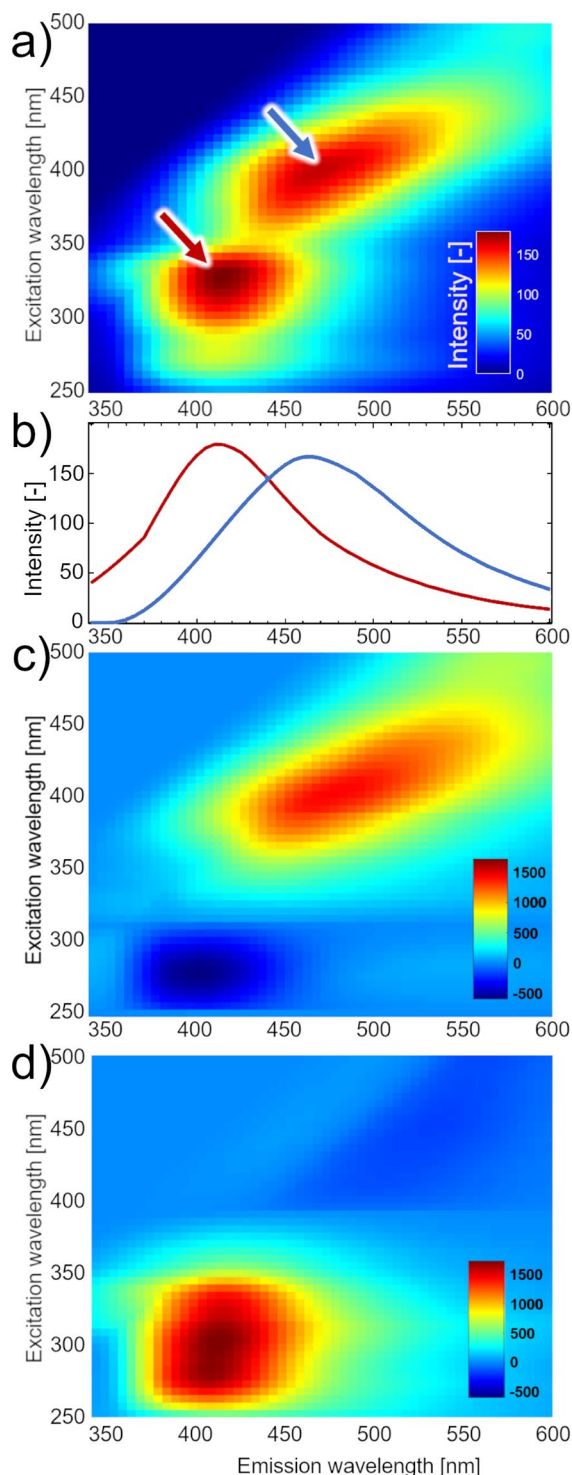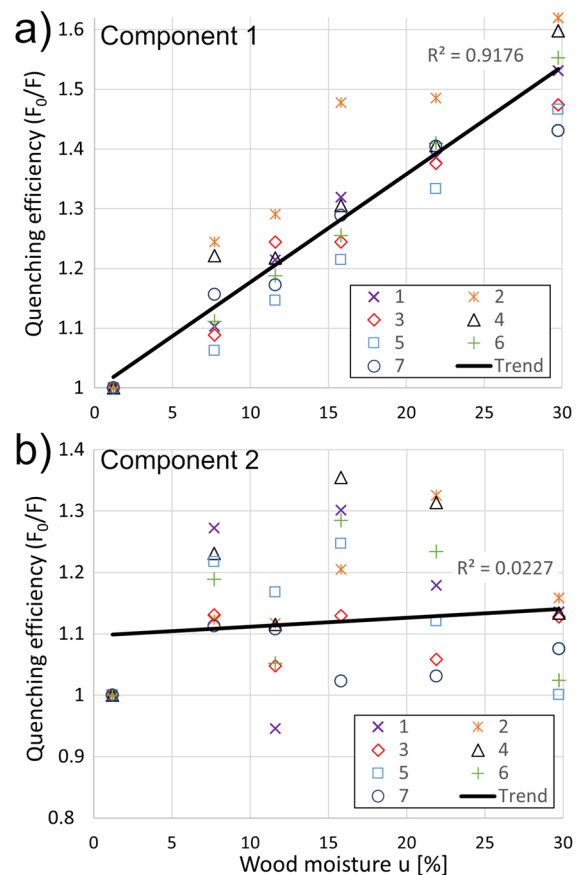
b show the quenching efficiency of the seven samples as a function of moisture content, also known as Stern–Volmer plot. Although some samples show
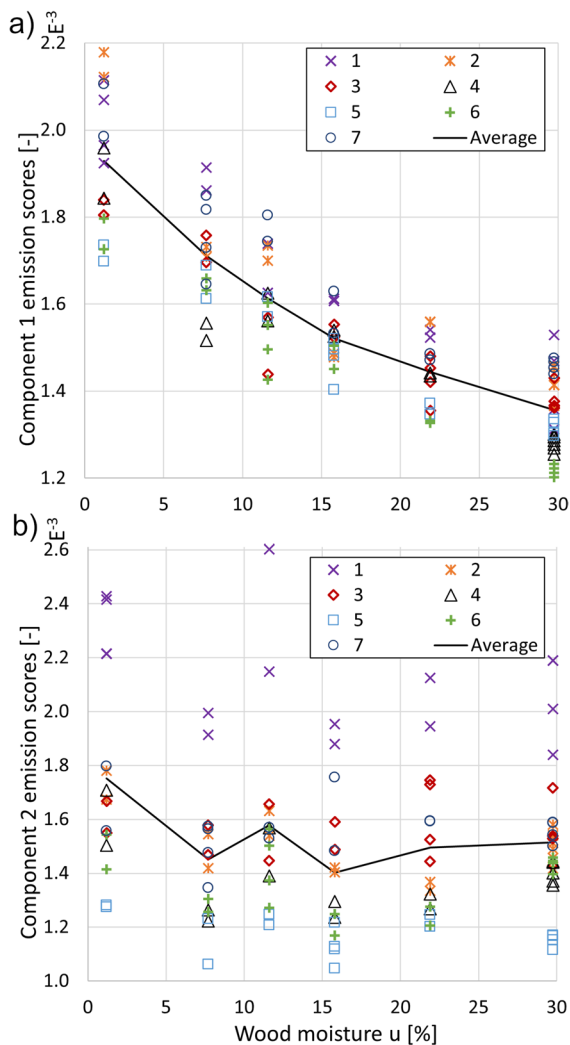
Fig. 2 Fluorescence intensity scores of component 1 (**a**) and component 2 (**b**) in samples 1–7, plotted against wood moisture. Samples were numbered in longitudinal order. All values relative to the respective kraft paper reference peak intensity

Fig. 3 Quenching efficiency (F_0/F) of components 1 (**a**) and 2 (**b**) as a function of moisture content, also known as Stern–Volmer plot. All values are mean values of the respective sample at the respective humidity stage

high variation, the overall trend is clearly pronounced and linear for component 1, while there is no clear trend for component 2.

The quenching effect by water was stronger at longer wavelengths. Figure 4a-c show the EEMs of the pine samples at 1.2% (F_0) and 29,8% (F) moisture content, and the quenching efficiency (F_0/F) EEM, respectively. The quenching efficiency (Fig. 4c) shows a clear maximum of 1.80 at Ex = 545 nm and Em = 635 nm, indicating that these fluorescence wavelengths were stronger quenched

by water. At Ex = 400; Em = 455, quenching efficiency had another maximum of 1.55, while the lower wavelengths (Ex < 370 nm) were only marginally quenched.

The mean excitation and emission maxima were both blue-shifted with increasing moisture content (Fig. 5a and b, respectively). Although the effect of moisture on peak excitation and emission wavelengths was not strong (rho = -0.41 and -0.29, respectively) and subject to statistical variation, the effect was significant according to Spearman's correlation analysis (p < 0.05 for Fig. 5a-c). Excitation and emission maxima of the lignocellulose peak were strictly correlated (rho = 0.93, Fig. 5c). This was present across all samples and moisture stages and represents an interesting feature.
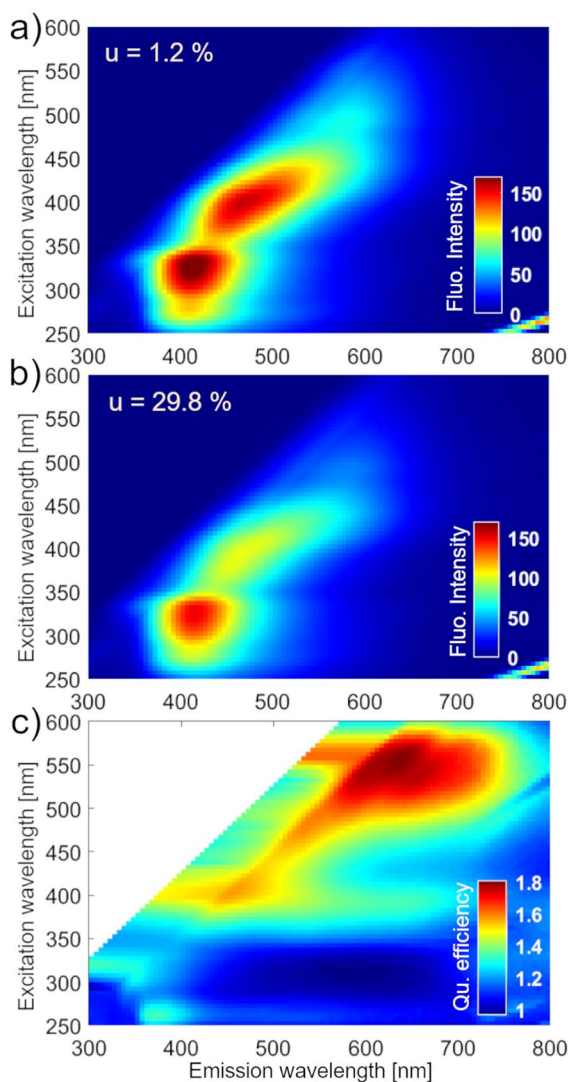
Fig. 4 Mean EEMs of samples at (**a**) 1.2 % and (**b**) 29.8 % moisture content, and (**c**) mean quenching efficiency EEM, calculated by dividing a) by b). High values in (**c**) express a strong quenching effect by water (the white area represents missing values due to division by zero)

Discussion

The peak at Ex = 385 and Em = 458 (component 1) was assumed to originate from the lignocellulose part of the wood, since wood fluorescence in this wavelength range was reported before in steam exploded lignocellulose (Auxenfans et al. 2017) and a variety of softwood and hardwood species like *Pinus radiata*, *Populus deltoides* (Donaldson 2013), and *Eucalyptus bosistoana* (Mishra et al. 2018). The peak at
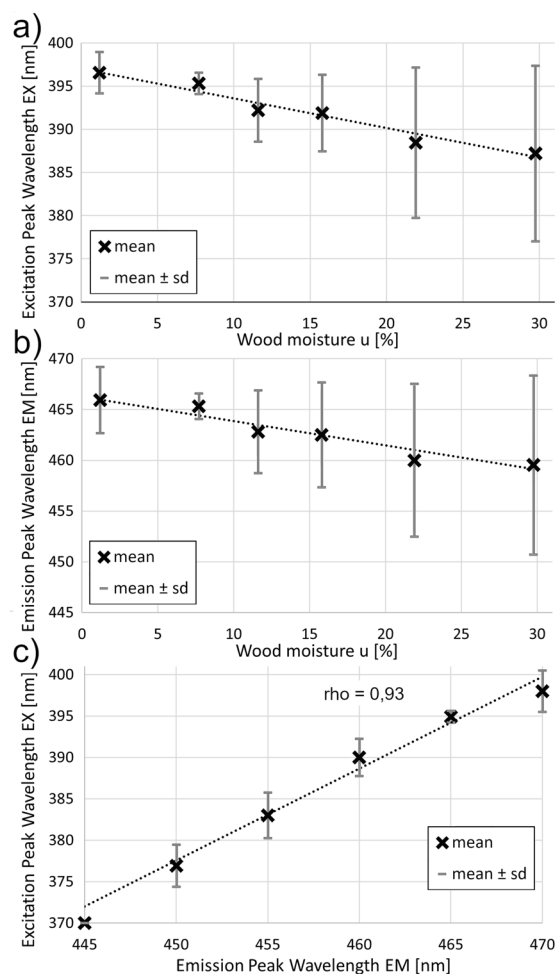
Fig. 5 Mean excitation (**a**) and emission (**b**) maxima of n = 112 EEMs, displayed against moisture content; (**c**) correlation between Ex and Em peak wavelengths. sd = standard deviation

Ex = 323 nm/Em = 413 nm (component 2) was attributed to pinosylvin and its monoethyl ether, two heartwood extractives of *Pinus sylvestris* L., as reported by Antikainen et al. (2012) and Belt et al. (2021).

Both the high between-sample variance and the high variance upon repeated measurement of the pinosylvin peak (Fig. 2b) were explained by an uneven distribution of pinosylvins in the wood. As reported by Belt et al. (2017), pinosylvin is present in extractive deposits in certain cell wall areas and lumina in Scots pine. Repeated placement in the spectrometer in a slightly different sample position caused the pinosylvin-rich areas to be in or out of the range of the excitation beam. This led to noise error in the intensity of pinosylvin fluorescence.

The diagonal shape of the lignocellulose peak (Fig. 1c), also called excitation-dependent emission, is an interesting feature, and a violation of Kasha's rule (Kasha 1950). It could be explained, for example, by the fact that a large number of different fluorophores are present in lignocellulose, with individual, overlapping fluorescence peaks. The diagonal peak could then be regarded as a sum of multiple overlapping peaks with small deviations in their excitation and emission energies. This is quite plausible in view of the chemical multiformity of lignin and hemicelluloses, but could also be explained by e.g. crystallite size or chain length of fluorescing carbohydrates. The dependence of cellulose fluorescence on crystallinity and chain length have been reported by Jiang et al. (2021) and Ding et al. (2020), respectively.

Theoretically, the shift could also be explained by the inner-filter effect and reabsorption, which is reported to cause a wavelength shift in high fluorophore concentrations, even in front-face geometry (Bevilacqua et al. 2020). However, the inner-filter effect seems to be irrelevant in this study, because the pinosylvin peak (Ex = 323 nm, Em = 413) did not show excitation-dependent emission. Because wood absorption is high in this wavelength range (Fengel and Wegener 2003), the inner-filter effect should be at least as strong for pinosylvin as for lignocellulose. However, it seemed to be not present for both.

The moisture quenching of lignocellulose (component 1 in Fig. 2a) indicates a strong interaction between the fluorescent substances and water.

Possible quenching mechanisms for water in solid wood are:

1. Quenching by energy transfer (energy loss) to water molecules
2. Suppression of Förster resonance energy transfer (FRET) between fluorophores through swelling
3. Suppression of clustering-triggered emission through swelling

Quenching by energy transfer (energy loss) to water molecules

In fluids, water is known to quench fluorescence of many organic dyes (Fürstenberg 2017; Maillard et al. 2020) by collisional quenching. In this mechanism, quenching efficiency is typically linearly correlated to quencher concentration, according to the Stern–Volmer-Equation (Stern and Volmer 1919). The linear Stern–Volmer plot of moisture quenching in wood (Fig. 3a) found in this study might support the hypothesis of collisional quenching by water.

Although collisional quenching is well-explained in fluids, some questions remain concerning the transferability to solids like wood. Collisional quenching requires the quenching molecule (liquid water) to collide with the fluorophore, leading to energy transfer to the water. However, below fibre saturation, water is more and more firmly bound to the cell wall through H-bonding (Thybring et al. 2022), and the energetic states of both water and lignocellulose change (Guo et al. 2016). At low moisture levels, other mechanisms than energy transfer to water might prevail.

Maillard et al. (2020) explained water quenching in 42 organic fluorophores by energy transfer to vibrational overtones of water, whereby the energy becomes unavailable for fluorescence. They argue that only the first layer of water molecules around the fluorophore are likely to contribute to the quenching effect. If water binds to wood in multiple layers at high moisture, as proposed by widespread sorption isotherm models (Hailwood and Horrobin 1946; Dent 1977; Skaar 1988), the quenching efficiency would be expected to flatten out when the monolayer capacity is reached. This was clearly not the case in this study (Fig. 3a).

In the recent years, the physical interpretations of these multilayer models have been questioned (Thybring et al. 2021). The observed linearity of the Stern–Volmer plot in this study indicates that within the hygroscopic range, each additional portion of water has the same potential of quenching lignocellulose fluorescence. This seems to support Willems (2014) who rejects the multilayer theories and proposes a sorption site occupancy (SSO) model instead (Willems 2015). According to the SSO model, all water molecules in the hygroscopic range directly bind to a sorption site in the cell wall matrix.

Maillard et al. (2020) found quenching mainly above 600 nm, and attributed it to the known overtones of water. This fits to the findings shown in Fig. 4c (dark red area in the upper right corner). The lower peak in Fig. 4c at Ex = 400 and Em = 455 cannot be explained by Maillard's hypothesis. Concludingly, energy transfer to vibrational states of water molecules can only explain part of the quenching observed in this study.

Suppression of energy transfer (FRET) between fluorophores through swelling

An alternative explanation of the moisture quenching of lignocellulose is the suppression of Förster Resonance Energy Transfer (FRET) between fluorophores through moisture swelling of the wood cell walls (increased distance between donor–acceptor pairs). FRET describes the transfer of excitation energy between a donor (short-wavelength absorber) and an acceptor (long-wavelength emitter) molecule. This mechanism is heavily influenced by the distance between the two molecules (Lakowicz 2006). Swelling of the wood cell wall as an effect of moisture uptake would result in longer distances and hence suppress this energy transfer, resulting in quenching of the long-wavelength acceptor fluorescence. If FRET takes place, the short-wavelength emission of the donor molecules is reduced, and the long-wavelength emission of the acceptor molecule appears instead. In other words: if FRET is suppressed, the total excitation and emission wavelengths of the mixture will be shorter. The blue-shift of excitation and emission peaks upon moisture uptake observed in this study (Fig. 5a-b) supports this hypothesis.

FRET donor and acceptor groups are likely to be present in wood. Terryn et al. (2020) used native wheat straw as FRET donor, in combination with rhodamine acceptor molecules. Native lignin contains a number of supposedly fluorescing groups (Donaldson 2020), and native cellulose is a mixture of diverse crystalline and amorphous areas of varying chain length. Both crystallinity (Du et al. 2019; Gong et al. 2013; Jiang et al. 2021; Kalita et al. 2015) and chain length (Ding et al. 2020) have been reported to influence the fluorescence emission of cellulose and other carbohydrates. Therefore, it seems likely that FRET takes place between various donor and acceptor units in wood at various wavelengths. The fact that the fluorescence emission maximum of lignocellulose shifts with excitation wavelength supports the presence of various fluorescent states, since pure compounds typically show excitation-independent emission spectra, according to Kasha's rule (Kasha 1950), which is a basic principle in photochemistry.

One feature of lignocellulose fluorescence remains unexplained by the FRET hypothesis: Ideally, the excitation peak of a fluorophore should be represented in its absorption spectrum, because the absorption of a photon is a requirement for fluorescence (Lakowicz 2006). However, according to literature (Sirviö et al. 2016; Zhang et al. 2020a; Ruwoldt et al. 2022), none of the wood cell wall polymers shows significant absorption peaks in the wavelength range around 385 nm, the excitation maximum observed in this study.

Suppression of clustering-triggered emission through swelling

Clustering-triggered and aggregation-induced fluorescence emission is a young research field, recently reviewed by Tomalia et al. (2019). In the recent years, lignin and cellulose fluorescence have repeatedly been reported to depend on clustering of certain functional groups in the solid state. Gong et al. (2013) found that cellulose and starch emit only in the solid state. Du et al. (2019) attributed the emission of cellulose and its derivatives to the clustering of ether, hydroxyl and carbonyl groups. Based on model calculations, Jiang et al. (2021) even found electron delocalisation in the crystalline states of celluloses I and II. Interestingly, the delocalisation of excitation energy in form of exciton waves in crystals was already reported by Zander (1981). Concerning lignin, Xue et al. (2016) stated that the suppression of intramolecular rotation through clustering of carbonyl groups leads to the solid state fluorescence emission of lignin.

In a recent review, Zhang et al. (2020b) identified the following six characteristic features of clustering-triggered luminogens:

1. their luminescence is based on non-conjugated molecular motifs, where *n-* or *pi-* electron-based groups are separated by nonconjugated linkers
2. the intrinsic luminescence of molecule clusters appears at longer wavelengths and independently of the *n-* or *pi-*electron-based luminescence in isolated states,
3. the excitation spectra appear red-shifted in comparison with their absorption spectra,
4. the emission profiles are excitation-dependent,
5. the emission profiles are size-dependent, with a higher molecular weight leading to a red-shift and an increase in emission, and

6. clustering-triggered luminogens are capable of phosphorescence.

Although Zhang et al. (2020b) admit that not all named characteristics are necessary requirements for clustering-triggered emission, lignocellulose shows all six properties, as discussed below:

1. Cellulose and other carbohydrates are known to fluoresce (Ding et al. 2020), although they do not contain conjugated molecular motifs. Carbohydrates are rich in hydroxyl (and partly carbonyl) groups that contain non-binding *n*-electrons. Lignin consists of aromatic structures that are separated by non-conjugated linkers (Mai and Zhang 2023).
2. The fluorescence of isolated aromatic structures in lignin occurs at lower wavelengths than the lignocellulose fluorescence observed in this study. Coniferyl alcohol fluorescence, for example, was reported at Ex = 310 nm and Em = 416 nm (Achyuthan et al. 2010), contrary to the lignocellulose peak at Ex = 385 nm and Em = 458 nm in this study (Fig. 1).
3. Lignin absorption peaks at app. 280 nm (Ruwoldt et al. 2022), while cellulose absorption lies below 200 nm (Sirviö et al. 2016). Both is much lower than the measured excitation maximum of 385 nm in this study.
4. The excitation-dependent emission profile of lignocellulose is shown in Fig. 1a.
5. Through water uptake, hydrogen-bonds between cell wall composites in wood become weaker and some eventually break (Thybring et al. 2022), thus reducing the effective cluster size and clustering-triggered emission intensity. Although Zhang et al. (2020b) limited the term "size" (5) to generations of dendrimers, molecular weight of polymers, diameter of nanoparticles etc., we propose that the weakening of hydrogen bonds within the clusters has a comparable effect to size reduction. In lignocellulose, this leads to a blue-shift (Fig. 5c) and a decrease (Fig. 3a) in emission, as observed in the present study.
6. Phosphorescence was not examined in this study, but reported for cellulose by Grönroos et al. (2018).

Concludingly, all six characteristic features of clustering-triggered emission are present in lignocellulose. Since clustering-triggered emission explains most of the characteristic (and uncommon) features of lignocellulose fluorescence, it seems reasonable to assume that its fluorescence originates from cluster-formation.

Conclusions

The exact mechanism for moisture quenching in wood may not be fully proved yet, but this study has shown for the first time that moisture quenching exists for wood, and that it follows a linear Stern–Volmer relationship. Contrary to widespread assumptions, carbohydrates do exhibit their own, independent fluorescence (Olmstead and Gray 1997). Since they have much more sorption sites for water than lignin (Fredriksson et al. 2023; Hou et al. 2022), it seems likely that the general fluorescence and the moisture quenching originate to a significant part from carbohydrates or an interaction between carbohydrates and lignin.

Clustering-triggered emission seems to best explain most of the quenching and wavelength shifting by water observed in this study.

PARAFAC2 proved to be a useful tool for modelling fluorescence peaks with excitation-dependent emission, i.e. lignocellulose fluorescence. It might be applied for spectral unmixing in further studies, for example to quantify fluorescent extractives in solid wood EEMs.

Declarations

Ethical approval Not applicable.

References

Achyuthan KE, Adams PD, Datta S, Simmons BA, Singh AK (2010) Hitherto unrecognized fluorescence properties of coniferyl alcohol. Molecules 15:1645–1667. https://doi.org/10.3390/molecules15031645

Antikainen J, Hirvonen T, Kinnunen J, Hauta-Kasari M (2012) Heartwood detection for Scotch pine by fluorescence image analysis. Holzforschung 66:877–881. https://doi.org/10.1515/hf-2011-0131

Atalla RH, Nagel SC (1972) Laser-induced fluorescence in cellulose. J Chem Soc Chem Commun 19:1049. https://doi.org/10.1039/C39720001049

Auxenfans T, Terryn C, Paës G (2017) Seeing biomass recalcitrance through fluorescence. Sci Rep 7:8838. https://doi.org/10.1038/s41598-017-08740-1

Avella T, Dechamps R, Bastin M (1988) Fluorescence Study of 10,610 Woody Species from the Tervuren (Tw) Collection, Belgium. IAWA J Int Assoc Wood Anatom 9:346–352. https://doi.org/10.1163/22941932-90001094

Babi M (2017) The Characterization of Cellulose Nanostructure using Super-Resolution Fluorescence Microscopy. Biophys J 112:144a. https://doi.org/10.1016/j.bpj.2016.11.793

Belt T, Keplinger T, Hänninen T, Rautkari L (2017) Cellular level distributions of Scots pine heartwood and knot heartwood extractives revealed by Raman spectroscopy imaging. Ind Crops Prod 108:327–335. https://doi.org/10.1016/j.indcrop.2017.06.056

Belt T, Venäläinen M, Harju A (2021) Non-destructive measurement of Scots pine heartwood stilbene content and decay resistance by means of UV-excited fluorescence spectroscopy. Ind Crops Prod 164:113395. https://doi.org/10.1016/j.indcrop.2021.113395

Bevilacqua M, Rinnan Å, Lund MN (2020) Investigating challenges with scattering and inner filter effects in front-face fluorescence by PARAFAC. J Chemom 34. https://doi.org/10.1002/cem.3286

Bro R, Andersson CA, Kiers HAL (1999) PARAFAC2-Part II. Modeling chromatographic data with retention time shifts. J Chemometrics 13:295–309. https://doi.org/10.1002/(SICI)1099-128X(199905/08)13:3/4%3c295::AID-CEM547%3e3.0.CO;2-Y

Camorani P, Badiali M, Francomacaro D, Gamassi M, Piuri V, Scotti F, Zanasi M (2008) A Classification Method for Wood Types using Fluorescence Spectra. In: 2008 IEEE Instrumentation and Measurement Technology Conference. I2MTC 2008] ; Victoria, BC, Canada, 12 - 15 May 2008. IEEE Service Center, Piscataway, NJ. 1312–1315.

Castellan A, Ruggiero R, Frollini E, Ramos LA, Chirat C (2007) Studies on fluorescence of cellulosics. Holzforschung 61:504–508. https://doi.org/10.1515/HF.2007.090

Chabbert B, Terryn C, Herbaut M, Vaidya A, Habrant A, Paës G, Donaldson L (2018) Fluorescence techniques can reveal cell wall organization and predict saccharification in pretreated wood biomass. Ind Crops Prod 123:84–92. https://doi.org/10.1016/j.indcrop.2018.06.058

Chimenez TA, Gehlen MH, Marabezi K, Curvelo AAS (2014) Characterization of sugarcane bagasse by autofluorescence microscopy. Cellulose 21:653–664. https://doi.org/10.1007/s10570-013-0135-9

Christensen GN, Kelsey KE (1959) Die Sorption von Wasserdampf durch die chemischen Bestandteile des Holzes. Eur J Wood Prod 17:189–203. https://doi.org/10.1007/BF02608811

Coletta VC, Rezende CA, Da Conceição FR, Polikarpov I, Guimarães FEG (2013) Mapping the lignin distribution in pretreated sugarcane bagasse by confocal and fluorescence lifetime imaging microscopy. Biotechnol Biofuels 6:43. https://doi.org/10.1186/1754-6834-6-43

Dent RW (1977) A Multilayer Theory for Gas Sorption. Text Res J 47:145–152. https://doi.org/10.1177/004051757704700213

Ding Q, Han W, Li X, Jiang Y, Zhao C (2020) New insights into the autofluorescence properties of cellulose/nanocellulose. Sci Rep 10:21387. https://doi.org/10.1038/s41598-020-78480-2

Djikanović D, Kalauzi A, Radotić K, Lapierre C, Jeremić M (2007) Deconvolution of lignin fluorescence spectra: A contribution to the comparative structural studies of lignins. Russ J Phys Chem 81:1425–1428. https://doi.org/10.1134/S0036024407090142

Donaldson L (2013) Softwood and Hardwood Lignin Fluorescence Spectra of Wood Cell Walls in Different Mounting Media. IAWA J 34:3–19. https://doi.org/10.1163/22941932-00000002

Donaldson L (2020) Autofluorescence in Plants. Molecules 25:2393. https://doi.org/10.3390/molecules25102393

Donaldson LA, Knox JP (2012) Localization of cell wall polysaccharides in normal and compression wood of radiata pine: relationships with lignification and microfibril orientation. Plant Physiol 158:642–653. https://doi.org/10.1104/pp.111.184036

Donaldson LA, Radotic K (2013) Fluorescence lifetime imaging of lignin autofluorescence in normal and compression wood. J Microsc 251:178–187. https://doi.org/10.1111/jmi.12059

Donaldson L, Vaidya A (2017) Visualising recalcitrance by colocalisation of cellulase, lignin and cellulose in pretreated pine biomass using fluorescence microscopy. Sci Rep 7:44386. https://doi.org/10.1038/srep44386

Donaldson LA, Kroese HW, Hill SJ, Franich RA (2015) Detection of wood cell wall porosity using small carbohydrate molecules and confocal fluorescence microscopy. J Microsc 259:228–236. https://doi.org/10.1111/jmi.12257

Du LL, Jiang BL, Chen XH, Wang YZ, Zou LM, Liu YL, Gong YY, Wei C, Yuan WZ (2019) Clustering-triggered Emission of Cellulose and Its Derivatives. Chin J Polym Sci 37:409–415. https://doi.org/10.1007/s10118-019-2215-2

Fengel D, Wegener G (2003) Wood: Chemistry, ultrastructure, reactions, Reprint der Orig.-Ausg. (ehem. de Gruyter) ed. Kessel, Remagen. https://doi.org/10.1002/pol.1985.130231112

Fredriksson M, Rüggeberg M, Nord-Larsen T, Beck G, Thybring EE (2023) Water sorption in wood cell walls–data exploration of the influential physicochemical characteristics. Cellulose 30:1857–1871. https://doi.org/10.1007/s10570-022-04973-0

Fürstenberg A (2017) Water in Biomolecular Fluorescence Spectroscopy and Imaging: Side Effects and Remedies. Chimia 71:26–31. https://doi.org/10.2533/chimia.2017.26

Galkin MV, Di Francesco D, Edlund U, Samec JSM (2017) Sustainable sources need reliable standards. Faraday Discuss 202:281–301. https://doi.org/10.1039/c7fd00046d

Gong Y, Tan Y, Mei J, Zhang Y, Yuan W, Zhang Y, Sun J, Tang BZ (2013) Room temperature phosphorescence from natural products: Crystallization matters. Sci China Chem 56:1178–1182. https://doi.org/10.1007/s11426-013-4923-8

Grönroos P, Bessonoff M, Salminen K, Paltakari J, Kulmala S (2018) Phosphorescence and fluorescence of fibrillar cellulose films. Nord Pulp Pap Res J 33:246–255. https://doi.org/10.1515/npprj-2018-3030

Guo X, Qing Y, Wu Y, Wu Q (2016) Molecular association of adsorbed water with lignocellulosic materials examined by micro-FTIR spectroscopy. Int J Biol Macromol 83:117–125. https://doi.org/10.1016/j.ijbiomac.2015.11.047

Hailwood AJ, Horrobin S (1946) Absorption of water by polymers: analysis in terms of a simple model. Trans Faraday Soc 42:B084. https://doi.org/10.1039/tf946420b084

Harshman RA (1972) PARAFAC2: Mathematical and technical notes. UCLA Work Paper Phon 22:30–44

Hoque M, Kamal S, Raghunath S, Foster EJ (2023) Unraveling lignin degradation in fibre cement via multidimensional fluorometry. Sci Rep 13:8385. https://doi.org/10.1038/s41598-023-35560-3

Hou S, Wang J, Yin F, Qi C, Mu J (2022) Moisture sorption isotherms and hysteresis of cellulose, hemicelluloses and lignin isolated from birch wood and their effects on wood hygroscopicity. Wood Sci Technol 56:1087–1102. https://doi.org/10.1007/s00226-022-01393-y

Ji Z, Ma JF, Zhang ZH, Xu F, Sun RC (2013) Distribution of lignin and cellulose in compression wood tracheids of Pinus yunnanensis determined by fluorescence microscopy and confocal Raman microscopy. Ind Crops Prod 47:212–217. https://doi.org/10.1016/j.indcrop.2013.03.006

Jiang J, Lu S, Liu M, Li C, Zhang Y, Yu TB, Yang L, Shen Y, Zhou Q (2021) Tunable Photoluminescence Properties of Microcrystalline Cellulose with Gradually Changing Crystallinity and Crystal Form. Macromol Rapid Commun 42:e2100321. https://doi.org/10.1002/marc.202100321

Kalita E, Nath BK, Deb P, Agan F, Islam MR, Saikia K (2015) High quality fluorescent cellulose nanofibers from endemic rice husk: Isolation and characterization. Carbohyd Polym 122:308–313. https://doi.org/10.1016/j.carbpol.2014.12.075

Kasha M (1950) Characterization of electronic transitions in complex molecules. Discuss Faraday Soc 9:14. https://doi.org/10.1039/df9500900014

Khalid A, Zhang L, Tetienne J-P, Abraham AN, Poddar A, Shukla R, Shen W, Tomljenovic-Hanic S (2019) Intrinsic fluorescence from cellulose nanofibers and nanoparticles at cell friendly wavelengths. APL Photonics 4:20803. https://doi.org/10.1063/1.5079883

Kiers HAL, ten Berge JMF, Bro R (1999) PARAFAC2-Part I. A direct fitting algorithm for the PARAFAC2 model. J Chemom 13:275–294. https://doi.org/10.1002/(SICI)1099-128X(199905/08)13:3/4%3c275::AID-CEM543%3e3.0.CO;2-B

Lakowicz JR (2006) Principles of fluorescence spectroscopy, 3rd ed. Springer, Boston. https://doi.org/10.1007/978-1-4757-3061-6

Leiter N, Wohlschläger M, Versen M, Laforsch C (2022) An algorithmic method for the identification of wood species and the classification of post-consumer wood using fluorescence lifetime imaging microscopy. J Sens Sens Syst 11:129–136. https://doi.org/10.5194/jsss-11-129-2022

Lloyd J, Miller JN (1979) Phosphorescence of adsorbed molecules at room temperature—the first observations? Talanta 26:180. https://doi.org/10.1016/0039-9140(79)80246-5

Ma T, Inagaki T, Tsuchikawa S (2023) Fit-free analysis of fluorescence lifetime imaging data using chemometrics approach for rapid and nondestructive wood species classification. Holzforschung 77:724–733. https://doi.org/10.1515/hf-2023-0017

Maceda A, Terrazas T (2022) Fluorescence Microscopy Methods for the Analysis and Characterization of Lignin. Polymers 14. https://doi.org/10.3390/polym14050961

Mai C, Zhang K (2023) Wood Chemistry. In: Springer Handbook of Wood Science and Technology, 1st ed. 2023 ed. Eds. Niemz, P., Teischinger, A., Sandberg, D. Springer International Publishing; Imprint Springer, Cham. 179–279. https://doi.org/10.1007/978-3-030-81315-4_5.

Maillard J, Klehs K, Rumble C, Vauthey E, Heilemann M, Fürstenberg A (2020) Universal quenching of common fluorescent probes by water and alcohols. Chem Sci 12:1352–1362. https://doi.org/10.1039/D0SC05431C

Mishra G, Collings DA, Altaner CM (2018) Cell organelles and fluorescence of parenchyma cells in Eucalyptus bositoana sapwood and heartwood investigated by microscopy. N.Z. J. of For. Sci. 48. https://doi.org/10.1186/s40490-018-0118-6.

Moya R, Wiemann MC, Olivares C (2013) Identification of endangered or threatened Costa Rican tree species by wood anatomy and fluorescence activity. Rev de Biol Trop 61:1113–1156. https://doi.org/10.15517/rbt.v61i3.11909

Olmstead JA, Gray DG (1997) Fluorescence Spectroscopy of Cellulose, Lignin and Mechanical Pulps: A Review. J Pulp Paper Sci : JPPS 23:J571

Pandey KK, Upreti NK, Srinivasan VV (1998) A fluorescence spectroscopic study on wood. Wood Sci Technol 32:309–315. https://doi.org/10.1007/BF00702898

Peters FB, Rapp AO (2021) Wavelength-dependent photodegradation of wood and its effects on fluorescence. Holzforschung 76:60–67. https://doi.org/10.1515/hf-2021-0102

Piuri V, Scotti F (2010) Design of an Automatic Wood Types Classification System by Using Fluorescence Spectra. IEEE Transactions on Systems, Man, and Cybernetics. Part C 40:358–366. https://doi.org/10.1109/TSMCC.2009.2039479

Rapp AO, Sudhoff B (2020) Schäden an Holzfußböden. 3. ed. Chapter 4.1.4., p. 84. Fraunhofer IRB Verlag, Stuttgart. https://doi.org/10.51202/9783738804300.

Ruwoldt J, Tanase-Opedal M, Syverud K (2022) Ultraviolet Spectrophotometry of Lignin Revisited: Exploring Solvents with Low Harmfulness, Lignin Purity, Hansen Solubility Parameter, and Determination of Phenolic Hydroxyl Groups. ACS Omega 7(50):46371–46383. https://doi.org/10.1021/acsomega.2c04982

Selig B, Luengo Hendriks CL, Bardage S, Daniel G, Borgefors G (2012) Automatic measurement of compression wood cell attributes in fluorescence microscopy images. J Microsc 246:298–308. https://doi.org/10.1111/j.1365-2818.2012.03621.x

Sirviö JA, Visanko M, Heiskanen JP, Liimatainen H (2016) UV-absorbing cellulose nanocrystals as functional reinforcing fillers in polymer nanocomposite films. J Mater Chem A 4:6368–6375. https://doi.org/10.1039/C6TA00900J

Skaar C (1988) Wood-water relations. Springer, Berlin

Stern O, Volmer M (1919) Über die Abklingungszeit der Fluoreszenz. Physikalische Zeitschrift 20:183–188

Terryn C, Habrant A, Paës G, Spriet C (2020) Measuring Interactions between Fluorescent Probes and Lignin in Plant Sections by sFLIM Based on Native Autofluorescence. J vis Exp. https://doi.org/10.3791/59925

Thybring EE, Boardman CR, Zelinka SL, Glass SV (2021) Common sorption isotherm models are not physically valid for water in wood. Colloids Surf, A 627:127214. https://doi.org/10.1016/j.colsurfa.2021.127214

Thybring EE, Fredriksson M, Zelinka SL, Glass SV (2022) Water in Wood: A Review of Current Understanding and Knowledge Gaps. Forests 13:2051. https://doi.org/10.3390/f13122051

Tomalia DA, Klajnert-Maculewicz B, Johnson KA-M, Brinkman HF, Janaszewska A, Hedstrand DM (2019) Non-traditional intrinsic luminescence: inexplicable blue fluorescence observed for dendrimers, macromolecules and small molecular structures lacking traditional/conventional luminophores. Prog Polym Sci 90:35–117. https://doi.org/10.1016/j.progpolymsci.2018.09.004

Werner T, Pecina H (1995) Versuche zur Anwendung der Fluoreszenz-Spektroskopie in der Holztechnologie für die Bewertung von Pilzbefall in Holz. Holz Als Roh- Und Werkstoff 53:49–55. https://doi.org/10.1007/BF02716387

Willems W (2014) The water vapor sorption mechanism and its hysteresis in wood: the water/void mixture postulate. Wood Sci Technol 48:499–518. https://doi.org/10.1007/s00226-014-0617-4

Willems W (2015) A critical review of the multilayer sorption models and comparison with the sorption site occupancy (SSO) model for wood moisture sorption isotherm analysis. Holzforschung 69:67–75. https://doi.org/10.1515/hf-2014-0069

Xue Y, Qiu X, Wu Y, Qian Y, Zhou M, Deng Y, Li Y (2016) Aggregation-induced emission: the origin of lignin fluorescence. Polym Chem 7:3502–3508. https://doi.org/10.1039/c6py00244g

Zander M (1981) Fluorimetrie. Springer, Berlin, Heidelberg

Zhang H, Wang X, Wang J, Chen Q, Huang H, Huang L, Cao S, Ma X (2020a) UV-visible diffuse reflectance spectroscopy used in analysis of lignocellulosic biomass material. Wood Sci Technol 54:837–846. https://doi.org/10.1007/s00226-020-01199-w

Zhang H, Zhao Z, McGoniga PR, Ye R, Liu S, Lam JWY, Kwok RTK, Zhang Yuan W, Xie J, Rogach AL, Tang BZ (2020b) Clusterization-triggered emission: Uncommon luminescence from common materials. Mater Today 32:275–292. https://doi.org/10.1016/j.mattod.2019.08.010